

UDC 624.072.2/4
IRSTI 67.11.35
RESEARCH ARTICLE

ANALYSIS OF I-BEAM WITH CORRUGATED WEB AND TECHNOLOGICAL PERFORATIONS UNDER STATIC LOAD

A.A. Bryantsev¹ , I.I. Ostapenko^{2,*} 

¹Scientific research institute «RAS Group Expert», 050062, Almaty, Kazakhstan

²International Educational Corporation, 050028, Almaty, Kazakhstan

Abstract. *The article is aimed at studying the operation of welded I-beams with corrugated web and technological perforations under static loading. The relevance of the study is due to the lack of specific instructions on the pitch, diameter and methods of strengthening technological perforations in the Republic of Kazakhstan and other countries. In this study the method of computer modeling with the help of the program complex LIRA-SAPR-2022 was used. The study was carried out for the beam, taking into account different sizes of perforations in the beam web, distances between the perforations, with and without perforation. The beam deformability and the beam stability with and without perforations under static concentrated load was analyzed. Twenty-nine beam models were analyzed, three circular perforations with diameters of $0,25h_w$, $0,5h_w$, $0,75h_w$ were formed in the webs of the beam models, where h_w is the height of the corrugated web. The center of the perforations was located in the middle of the web height. The distance between the centers of the perforations were taken $2d$, $3d$ and $4d$, where d is the diameter of the perforation. Analysis of the performance of beam models with perforations under load showed that the bearing capacity of the beam decreases with increasing perforation pitch and perforation diameter. The most optimum perforation diameter for design may be perforation diameter $0,25h_w$ and $0,5h_w$ with perforation pitch $2d$.*

Keywords: *Beam with corrugated web, circular perforation, beam deformability, bearing capacity, beam stability, concentrated load.*

***Corresponding author**

Ostapenko Inna Ivanovna, e-mail: ostapinna@mail.ru

<https://doi.org/10.51488/1680-080X/2024.3-05>

Received 05 February 2024; Revised 21 May 2024; Accepted 30 May 2024

СТАТИКАЛЫҚ ЖҮКТЕМЕ КЕЗІНДЕ ГОФРЛЕНГЕН ҚАБЫРҒАЛАРЫ ЖӘНЕ ТЕХНОЛОГИЯЛЫҚ САҢЫЛАУЛАРЫ БАР ҚОС ТАВРЛЫ АРҚАЛЫҚТЫҢ ЖҰМЫСЫН ТАЛДАУ

А.А. Брянцев¹ , И.И. Остапенко^{2*} 

¹ Ғылыми-зерттеу институты «RAS Group Expert», 050062, Алматы, Қазақстан

² Халықаралық білім беру корпорациясы, 050028, Алматы, Қазақстан

Андатпа. Бұл зерттеу статикалық жүктеме кезінде гофрленген қабырғалары мен технологиялық саңылаулары бар дәнекерленген екі таврлы арқалықтардың жұмысын зерттеуге бағытталған. Зерттеудің өзектілігі Қазақстан Республикасының аумағында және басқа елдерде технологиялық саңылаулардың қадамы, диаметрі және нығайту әдістері туралы нақты нұсқаулардың болмауына байланысты. Зерттеуде LIRA-SAPR-2022 бағдарламалық пакетін пайдаланып, компьютерлік модельдеу әдісі қолданылды. Зерттеу арқалық қабырғасындағы саңылаулардың әртүрлі өлшемдерін, саңылаулар арасындағы қашықтықты ескере отырып, саңылауды күшейту және күшейтусіз жүргізілді. Статикалық шоғырланған жүктеме әсерінен саңылаулары бар және саңылаулары жоқ арқалықтың көтергіштігі мен тұрақтылығы зерттелді. Компьютерлік модельдеу соңғы элементтер әдісін қолдану арқылы LIRA-SAPR бағдарламалық кешенінің көмегімен жүргізілді. Осы бағдарламалық кешеннің көмегімен арқалықтардың 29 моделі зерттелді. Арқалық модельдердің қабырғасында диаметрі $0,25h_w$, $0,5h_w$, $0,75h_w$ болатын үш дөңгелек саңылау пайда болды, мұнда h_w - гофрленген қабырғаның биіктігі. Тесіктердің ортасы қабырға биіктігінің ортасында орналасқан. Саңылау орталықтары арасындағы қашықтық $2d$, $3d$ және $4d$ қабылданады, мұндағы d - саңылаудың диаметрі. Шоғырланған жүктеме астындағы саңылаулары бар арқалық модельдерінің жұмысын талдау саңылау қадамы мен саңылау диаметрінің ұлғаюымен арқалықтың көтергіштігі төмендейтінін көрсетті, жобалау кезінде ең оңтайлы саңылау диаметрі $0,25h_w$ және $0,5h_w$ саңылау қадамы $2d$ қабылданады.

Түйін сөздер: гофрленген қабырғасы бар арқалық, дөңгелек саңылау, арқалықтың деформативтілік, жүк көтергіштігі, арқалықтың тұрақтылығы, шоғырланған жүктеме

* Автор-корреспондент

Остапенко Инна Ивановна, e-mail: ostapinna@mail.ru

<https://doi.org/10.51488/1680-080X/2024.3-05>

Алынды 05 ақпан 2024; Қайта қаралды 21 мамыр 2024; Қабылданды 30 мамыр 2024

УДК 624.072.2/4

МРНТИ 67.11.35

ИССЛЕДОВАТЕЛЬСКАЯ СТАТЬЯ

АНАЛИЗ РАБОТЫ ДВУТАВРОВОЙ БАЛКИ С ГОФРИРОВАННОЙ СТЕНКОЙ И ТЕХНОЛОГИЧЕСКИМИ ОТВЕРСТИЯМИ ПРИ СТАТИЧЕСКОЙ НАГРУЗКЕ

А.А. Брянцев¹ , И.И. Остапенко^{2*} 

¹ Научно-исследовательский институт «RAS Group Expert»

² Международная образовательная корпорация, Алматы, 050028, Казахстан

Аннотация. Статья направлена на изучение работы сварных двутавровых балок с гофрированными стенками и технологическими отверстиями при статической нагрузке. Актуальность исследования обусловлена отсутствием на территории Республики Казахстан и на территории других стран конкретных указаний о шаге, диаметре и методах усиления технологических отверстий. В исследовании использован метод компьютерного моделирования при помощи программного комплекса ЛИРА-САПР-2022. Исследование проводилось для балки, с учетом различных размеров отверстий в стенке балки, расстояний между отверстиями, с усилением и без усиления отверстия. Исследовалась несущая способность и устойчивость балки с отверстием и без отверстий под действием статической сосредоточенной нагрузки. Было исследовано 29 моделей балок, в стенках моделей балок образовывались три круглых отверстия диаметром $0,25h_w$, $0,5h_w$, $0,75h_w$, где h_w – это высота гофрированной стенки. Центр отверстий располагался посередине высоты стенки. Расстояние между центрами отверстий приняты $2d$, $3d$ и $4d$, где d – это диаметр отверстия. Анализ работы моделей балок с отверстиями под нагрузкой показал, что с увеличением шага отверстий и диаметра отверстий несущая способность балки понижается. Наиболее оптимальным диаметром отверстия при проектировании может быть отверстие диаметром $0,25h_w$ и $0,5h_w$ с шагом отверстий $2d$.

Ключевые слова: балка с гофрированной стенкой, круглое отверстие, деформативность балки, несущая способность, устойчивость балки, сосредоточенная нагрузка.

*Автор–корреспондент

Остапенко Инна Ивановна, e-mail: ostapinna@mail.ru

<https://doi.org/10.51488/1680-080X/2024.3-05>

Поступило 05 февраля 2024 г.; Пересмотрено 21 мая 2024 г.; Принято 30 мая 2024 г.

ACKNOWLEDGEMENTS/SOURCE OF FUNDING

The study was conducted using private sources of funding.

CONFLICT OF INTEREST

The authors state that there is no conflict of interest.

АЛҒЫС/ҚАРЖЫЛАНДЫРУ КӨЗІ

Зерттеу жеке қаржыландыру көздерін пайдалана отырып жүргізілді.

МҮДДЕЛЕР ҚАҚТЫҒЫСЫ

Авторлар мүдделер қақтығысы жоқ деп мәлімдейді.

БЛАГОДАРНОСТИ/ИСТОЧНИК ФИНАНСИРОВАНИЯ

Исследование проводилось с использованием частных источников финансирования

КОНФЛИКТ ИНТЕРЕСОВ

Авторы заявляют, что конфликта интересов нет.

1 INTRODUCTION

In accordance with Kazakhstani normative documents, it is recommended to use transverse corrugated web in beams to increase their stability and reduce the mass of the structure. When making calculations, it is necessary to check local and overall stability of rectangular compartments of the corrugated web of the beam. In addition, tangential stresses and deflection of the beam are important parameters in the calculation of beams with corrugated web. When analyzing in detail the European and Russian standards for design and calculation of beams with corrugated wall, it is possible to find similarities and differences in the designations of coefficients and other values.

Factors affecting the bearing capacity of a beam with corrugated web weakened by perforations:

1. Location of the perforation in the beam in relation to its most dangerous zones of stress concentration (for example, in sections near the supported ones);
2. The perforations pitch in the web of the beam along its length;
3. Shape of the perforation (for example, a square, rectangular or the most common circular perforation);
4. Flexibility of the web;
5. The perforation center in relation to the web height.

The need for perforations application in the corrugated webs is due to the fact that laying of the piping system for various purposes: water supply, heating, ventilation, air conditioning, etc. is necessary in accordance with Operational Requirements.

The basic forms of stability loss of beams corrugated webs:

- local loss of stability of the web under a concentrated load reflecting the nature of its operation under the girder, in the case of beams with corrugated webs instead of trusses;
- local loss of stability of a separate panel of corrugations between their peaks. This loss of local stability of the corrugated web in appearance and in essence of its operation is similar to the loss of local stability of a flat web between vertical stiffeners;
- general loss of stability of the corrugated web in the zones of action of the maximum shearing stresses. This loss of general stability of the corrugated web in appearance and in essence of its operation is similar to the loss of general stability of a flat web supported by vertical stiffeners with insufficient bending stiffness.

Basically, beams with a cross-corrugated web and triangular-shaped corrugations are used for construction in Kazakhstan (**Figures 1**);



Figure 1 – Beams with cross-corrugated web and triangular-shaped corrugations: L_r – is the length of the corrugation half-wave; f_r – is the height of the corrugation half-wave (the authors' material).

– beams with a cross-corrugated web and corrugations of a trapezoidal shape are used in Sweden and the USA (**Figures 2 and Figures 3**);

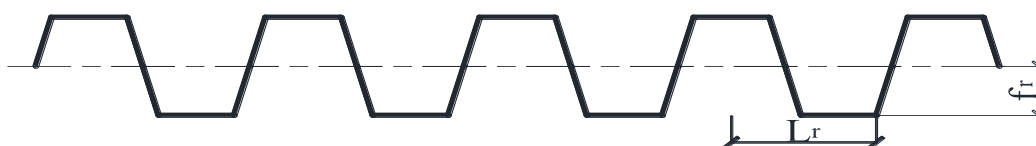


Figure 2 – Beams with corrugations of a trapezoidal shape: L_r – is the length of the corrugation half-wave; f_r – is the height of the corrugation half-wave (the authors' material).

– beams with a cross-corrugated web and corrugations of a rectangular shape are used in Finland, Japan and the Netherlands;

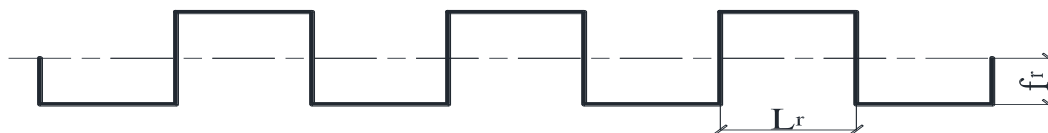


Figure 3 – Beams with corrugations of a rectangular shape: L_r – is the length of the corrugation half-wave; f_r – is the height of the corrugation half-wave (the authors' material).

– beams with a cross-corrugated web and wavy-shaped corrugations are used in Austria, Ukraine, Poland and Russia (**Figures 4**).



Figure 4 — Beams with cross-corrugated web and wavy-shaped corrugations: L_r – is the length of the corrugation half-wave; f_r – is the height of the corrugation half-wave (the authors' material).

Corrugation is the process of folds (corrugations) formation by folding a sheet in sheet materials, in a certain distance necessary for enhancement of the material characteristics: strength and stability.

2 LITERATURE REVIEW

The corrugated I-beam has the shape of the letter “H” and consists of two belts of arbitrary metal profile and a corrugated web. The web can be made with different corrugations profiles: triangular, wave-shaped, trapezoidal, rectangular and others. The girders of such a beam are usually made of rolled metal, bent steel sections, welded pipes or reinforced concrete elements (**Bryantsev 2017**).

Corrugated structures have become widely used in the shipbuilding industry at the end of the 19th and early 20th centuries, in the 1930s in the aircraft industry.

According to the research of **Poltoradnev (2013)**, the performance of a beam with a peppered-corrugated wall can be divided into four stages:

- 1) Stage of subcritical operation;
- 2) Stage of supercritical operation,
- 3) Stage of elastoplastic behavior of the section in the load zone;
- 4) Bearing-capacity failure stage.

Field of use of corrugated structures is extensive: they are used as load-bearing structures for floor beams and coverings in residential, public, administrative and industrial buildings.

In 1928, **Tuzi (1928)** made a comparative analysis of the stress distribution between the experimental data on the effect of a circular perforation centered on the neutral axis of a flat beam web affected by bending moment and the results of stress distribution theory.

Cocker et al. (1936) in his work conduct a research on the distribution of stresses in a tension plate with one or more perforation. He investigated the effect of unbalanced forces applied to the contour of perforation in a flat plate.

The issues of the openings effect on the work of the beam web which are performed according to the Vierendeel principle or the four-angular bend (**Kudryavtsev 2011**), are studied in various works by **Chung (2001, 2003)**, **Darwin (1990)**, **Hagen (2009)**, **Shanmugan et al. (2002)**, **Ibrahim (1999)**, **Ahmed, M.S. (2022)**.

Also, the problems of placing and stiffening of openings in the corrugated webs of trapezoidal and wavy shape of corrugations were solved in different countries by many scientists. For ex-

ample, Romeijn) et al. (2009), Kiyamaz, et al. (2010), Chittaranjan et al (2019), Amr et al (2021), Ahmed, et al (2022).

The scientific paper (Bryantsev, 2019) presents tests that was performed on large-scale models (scale 1:3) of welded I-beams of constant section (flange is 200×10mm, web is 840×1.9mm) with span of 8,400 mm. The first beam without perforations B-1. Three circular perforations with a diameter of 380 mm, which edges were reinforced with stiffness elements made of strip steel with a cross section of 85×3mm, are formed in the web of the second beam B-2. The maximum allowable deflection of the beam is assumed to be $\frac{1}{220L}$ or 38.2 mm.

The paper (Bryantsev, 2020) presents experimental studies of welded I-beams with corrugated web. The main purpose of the study was to conduct laboratory tests of welded I-beams with corrugated webs weakened by two technological circular perforations with different ways of their stiffening in, as well as to determine the most effective way of stiffening the circular perforations. It is necessary to perform a comparative analysis of experimental and computer data of beam deflections, to study the peculiarity of limit states and the behavior of models under load, to determine the maximum bearing capacity and ultimate deflection of the models under consideration. Within the framework of the conducted research, five variants of corrugated beams were considered, having the same length, height and web thickness, perforation diameters, as well as height and wavelength of the corrugation, but differing in the absence and presence of perforations, as well as methods of their stiffening.

3 MATERIALS AND METHODS

While performing this scientific research the theoretical method of studying the posed scientific questions was used. To write the article, the results obtained were systematized and presented in an accessible and understandable form.

The theoretical methods of scientific research are presented in the article in the form:

- analysis, used to study in detail the use of beams with cross-corrugated web and triangular-shaped corrugations weakened by circular perforations;
- modeling, used in the form of numerical parametric study of 29 models of beams, including beams with triangular corrugation and thin-walled ribbed beams, performed in the LIRA-SAPR 2022 software package.

A numerical parametric study was performed on a welded corrugated beam with the corrugations of triangular shape; the model and testing of such beam is described in paragraph 2.1. Numerical simulation of the beams was performed using the LIRA-SAPR 2022, general-purpose program for the finite element analysis, which includes the requirements for constructions in accordance with Eurocode 3 Part 1.5-Plated Structural Elements. This program can be used to solve various tasks, from simple linear analysis and on out to complex nonlinear analysis requiring consideration of various manufacturing deviations and material errors. The parametric study was performed for the beam taking into account the various sizes of the perforations in the beam web, distances between the perforations, existence and absents of the perforation stiffening, as well as for the corrugated beam with no web perforations. The ability of the beam web with and without the perforation to withstand the load was considered and an assessment of the effect of web flexibility in accordance with Eurocode 3 Part 1.5-Plated Structural Elements was performed.

The tested beam has three perforations; the perforations' centers are located in the middle of the web height. The distance between the centers of the perforations is assumed to be $2d$, $3d$ and $4d$. One of the perforations has a constant location in the center of the beam at a distance of 4.2 m from the left and right support to the opening center. As for the geometric parameters of the perforation, a circular shape of the perforation was used. The perforations of three different sizes were used during the parametric study.

Also, for comparative analysis, a model of a thin-walled rib girder with similar dimensions was developed. The web is stiffened only by transverse ribs, the width of their projecting part b_h for

a pair of symmetric ribs is not less than $h_{ef}/30+40$ mm. But, since in practice, more often used ribs, completely filling the cross-section of the beam, it is assumed $b_h = b_{ef}$, and the thickness of the rib t_s not less than $2b_h \sqrt{\frac{R_y}{E}}$, we take 20mm. The distance between the main cross ribs shall not exceed $2h_{ef}$ when $\lambda_{\bar{\lambda}_w} > 3,2$ and $2,5 h_{ef}$ when $\lambda_{\bar{\lambda}_w} \leq 3,2$. Since $\lambda_{\bar{\lambda}_w} = 15,25$ we take the distance between the stiffening ribs $2h_{ef}$ i.e. 2×840 mm = 1680 mm.

The boundary conditions were applied to both ends of the beam model at the nodes of the end plate surface by limiting the required degrees of freedom. For the adopted models, the resistance to deformation values was assumed to be 245 MPa, the elastic modulus $E = 206,000$ MPa and the Poisson ratio is 0.3, the design buckling resistance $R_s = 142.1$ MPa. For a beam models with the length of 8,400 mm, the maximum allowable deflection is $1/220l$ or 38.2 mm. Loading (Q) of models is from 50 kN to 350 kN. Loading step is 50 kN.

Numerical parametric study of the beams with cross-corrugated web and triangular-shaped corrugations includes analysis of basically 29 finite element models. Of these 29 models, 2 beam model with no web perforations and 27 models with perforations of different sizes in the design, as indicated above; and they are located at different distances from each other. The thickness of corrugated web t_w is 1.9 mm.

When computer simulation the beam with a web height h_w of 840mm and a web thickness t_w of 1.9mm was used. The wavelength of web corrugations of triangular shape is l_r 350 mm and a wave height f_r is 54 mm (fig.1). The material of the web and flanges is C245 steel (Figures 5).



The corrugation thickness t_w is 1.9 mm
The corrugation wavelength L_r is 350 mm;
The corrugation height f_r is 54 mm.

Figure 5 — Values of length, height and thickness of the triangular-shaped corrugations adopted in computer modeling (authors' material).

Finite element models adopted for beams with the corrugations of triangular shape with and without perforations are given in Figures 6.

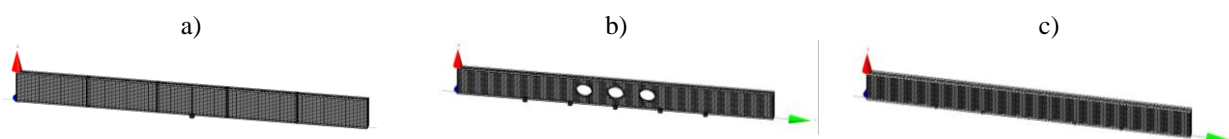


Figure 6 – Models adopted for the analysis of beams, where (a) flat web beam supported by stiffeners; (b) welded I-beam with cross-corrugated web and triangular-shaped corrugations weakened by perforations; (c) welded I-beam with cross-corrugated web and triangular-shaped corrugations without corrugations (authors' material).

Welded I-beam of constant section (flanges are 200×10 mm, webs are $840 \times 1,9$ mm) with span of 8,400 mm. Three circular perforations with the diameter of $0.25h_w$, $0.5h_w$, $0.75h_w$ are formed in the beam web. In the first case, perforations are made without edging with sheet steel. In the second case, the perforations are stiffened with strip steel in the area equal to the perforations area with a thickness $t = 3$ mm and a width of 50 mm for perforation of $0.25h_w$ in diameter, 110 mm in width for perforation of $0.5h_w$ in diameter, 180 mm in width for perforation with a diameter of $0.75h_w$. In the third case, the perforations are supported by stiffness elements of strip steel in the area of the same perforation area, with a thickness $t = 3$ mm and width, as in the second case, as

well as paired vertical stiffeners of bar steel with a section of 85×3 mm. Two end plates with a thickness $t = 20$ mm at the ends of each model.

The load is applied through a rigid rectangular pipe of length $l = 200$ mm, which is in direct contact with the surface of the shelf. The load is transmitted at five points from the bottom to the top. The load is applied in the beam center, as well as at a distance from the center in both directions of 1.2 m in accordance with the model loading diagrams (Figure 7).

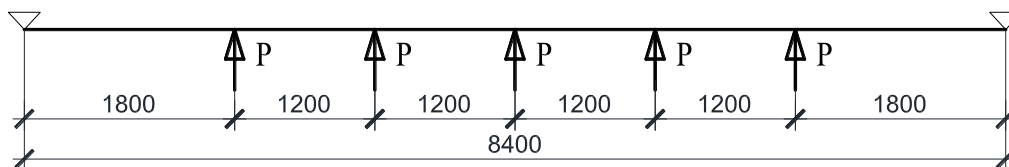


Figure 7 – Model loading diagram for parametric study (authors' material).

In general, **all** models show reduction in resistance of the elements to loss of stability with increase of the perforation size. Therefore, to decrease the deflections and increase the stability and strength of the beam weakened by the perforations it is necessary to stiffen the perforation. Analysis of operation of the beam models with perforations under a concentrated load showed reduction of the beam bearing capacity with an increase of the perforations pitch from $2d$ to $4d$ and the diameter of the openings from $0.25h_w$ to $0.75h_w$. The most optimal diameter of the perforation when designing can be the diameter of the opening of $0.25h_w$ and $0.5h_w$ with $2d$ or $3d$ openings pitch. Stiffening the perforation by edging with sheet steel, as well as the perforation stiffening with paired vertical stiffeners is necessary to increase the load-bearing capacity of the corrugated I-beam weakened by perforations. In the case of an acute need of the perforation with a diameter of $0.75h_w$ it is recommended to use steel with higher strength characteristics in order to increase the bearing capacity and reduce the laboriousness of its manufacture.

4 RESULTS AND DISCUSSIONS

Results of computer modeling of beam with cross-corrugated web and triangular-shaped corrugations and with perforations in the web

Figure 8 shows the load-deflection dependence of the middle of the M-1 and M-2 beam models in the elastic stage.

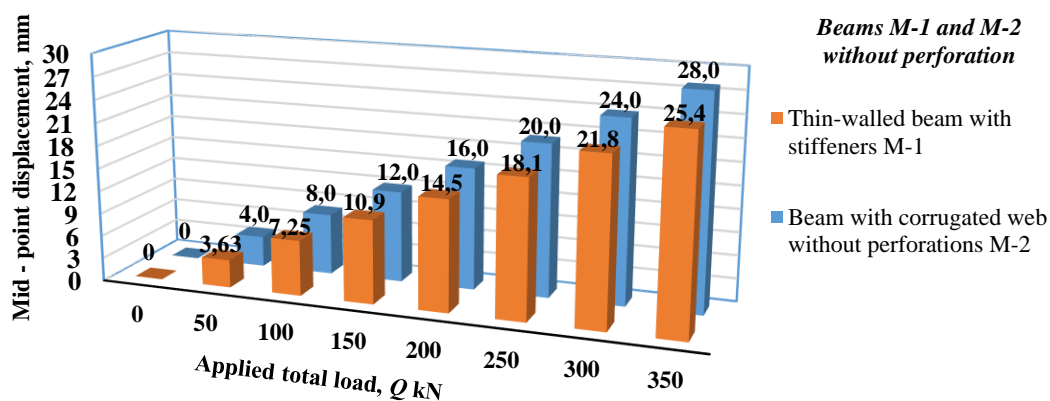


Figure 8 – The plot of displacement and applied total load value dependence for the M-1 and M-2 beam models (authors' material).

Analyzing the obtained data for the beam models we see that the maximum allowable deflection is not reached and for the beam model M-1 it is 25.4 mm, and for the beam model M-2 it is 28 mm. The deflection of the corrugated girder is 9.3% higher than that of the girder with a flat web.

The maximum experimental load is usually higher for the corrugated beam model than for the thin-walled beam model of the same thickness, with their flexibility equal to or greater than 90, which confirms the economic efficiency of their use in construction in general, and in earthquake-resistant construction in particular, due to the increased reliability of their performance under load. In our case, the applied maximum experimental load for the model of a beam with a corrugated wall and for the model of a thin-walled beam supported by stiffeners of the same thickness have approximately the same values, but the reliability of the model of a beam with a corrugated web and in this case is much higher than that of the model of a thin-walled beam, which is another factor in justifying their wide application in earthquake-resistant construction.

The **Figure 9** shows the load-deflection dependence of the middle of the M-2, M-3 and M-4 beam models with $2d$ perforation pitch in the elastic stage.

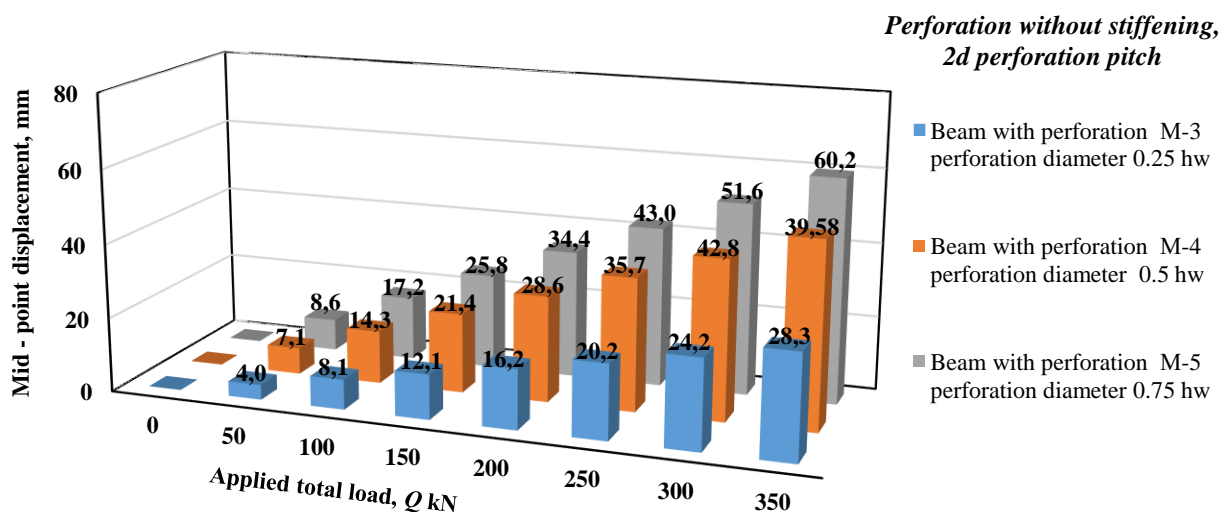


Figure 9 – The plot of displacement and applied total load value dependence for the M-3, M-4 and M-5 with $2d$ perforation pitch without perforation stiffening (authors' material).

In order to determine the most efficient variant of the corrugated beam model with perforations, it was decided to start analyzing the corrugated beam models with $2d$ perforation pitch without perforation stiffening. The obtained data allow us to conclude that the best result was shown by the model M-3 with the perforation diameter $0.25h_w$, the maximum displacements of which do not exceed the permissible ones. All the models show decreasing values of resistance of elements to loss of stability with increasing perforation size. Therefore, to reduce the deflections and increase the stability and strength of the beam weakened by perforations, perforation stiffening is necessary.

The **Figure 10** shows the load-deflection dependence of the middle of the M-6, M-7 and M-8 beam models with $2d$ perforation pitch in the elastic stage.

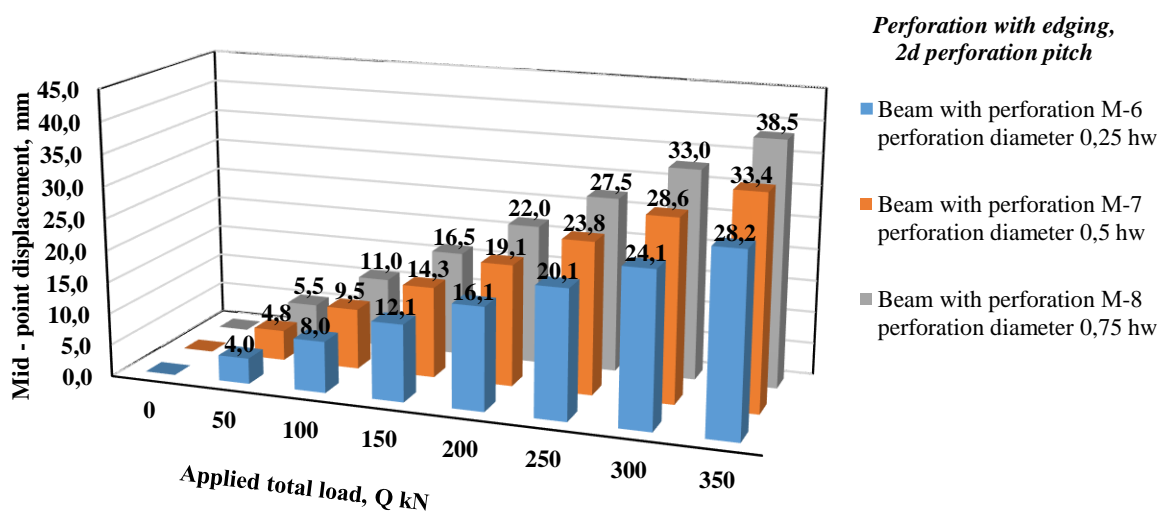


Figure 10 – The plot of displacement and applied total load value dependence for the M-6, M-7 and M-8 with 2d perforation pitch with perforation border (authors' material).

Analysis of the obtained data of M-6, M-7 and M-8 beam models with 2d perforation pitch and 3 mm thick strip steel perforation edging generally shows better results than without perforation stiffening.

The **Figure 11** shows the load-deflection dependence of the middle of the M-9, M-10 and M-11 beam models with 2d perforation pitch in the elastic stage.

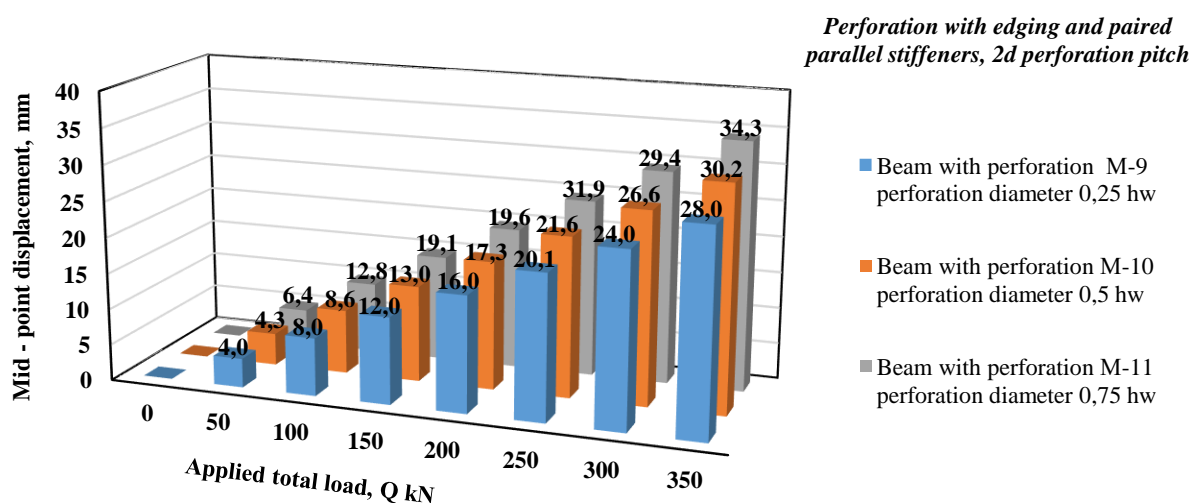


Figure 11 – The plot of displacement and applied total load value dependence for the M-9, M-10 and M-11 with 2d perforation pitch with perforation edging and paired parallel stiffeners (authors' material).

The final step in strengthening the beam models with 2d perforation pitch was the incorporation of paired parallel stiffeners in the work of the perforation web stiffened with edging. The stiffener thickness was assumed to be 10 mm. For beam model M-9 with perforation diameter $0.25h_w$, strengthening with paired ribs had almost no effect on its bearing capacity, but for beam models M-10 and M-11 with perforation diameters $0.5h_w$ and $0.75h_w$ showed better results.

The **Figure 12** shows the load-deflection dependence of the middle of the M-12, M-13 and M-14 beam models with 3d perforation pitch in the elastic stage.

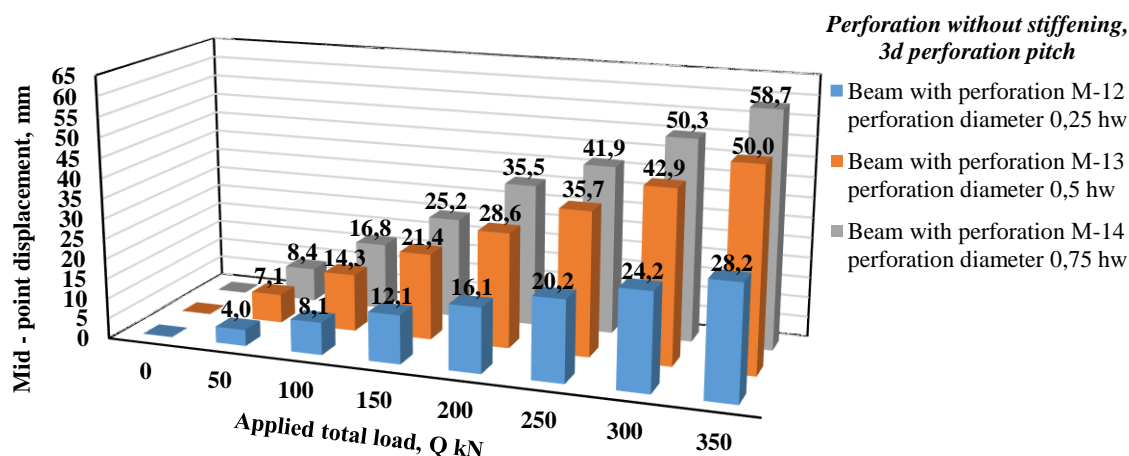


Figure 12 – The plot of displacement and applied total load value dependence for the M-12, M-13 M-14 with 3d perforation pitch without perforation stiffening (authors' material).

Analyzing the obtained data of beam models M-12, M-13 and M-14 it can be concluded that in general the deflections and deformations of beam models with 3d perforation pitch without perforation reinforcement are larger than those of similar beam models M-3, M-4, M-5 with the same perforation diameter but different 2d perforation pitch. The deformations and displacements of beam models M-12 and M-3 with 3d and 2d perforation pitch and perforation diameter $0.25h_w$, are identical.

The **Figure 13** shows the load-deflection dependence of the middle of the M-15, M-16 and M-17 beam models with 3d perforation pitch in the elastic stage.

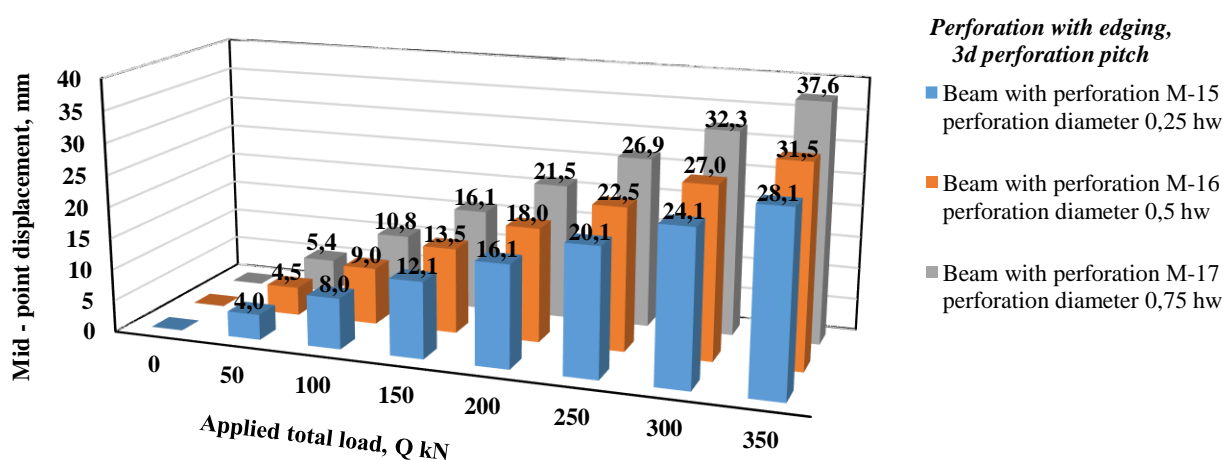


Figure 13 – The plot of displacement and applied total load value dependence for the M-15, M-16 and M-17 with 3d perforation pitch with perforation border (authors' material).

After the performance of beam models M-15, M-16 and M-17 with 3d c perforation pitch was included with perforation stiffening by edging, the following results were obtained: as in the previous cases, the behavior of model M-15 with perforation diameter $0.25h_w$ and 3d perforation pitch showed little change after the stiffening and also showed almost no change compared to the data obtained for model M-6 with the same diameter but perforation pitch equal to 2d. But for the other two models M-16 and M-17, the fringing reinforcement had a positive effect and reduced their deflection compared to the beam models M-13 and M-14.

The **Figure 14** shows the load-deflection dependence of the middle of the M-18, M-19 and M-20 beam models with 3d perforation pitch in the elastic stage.

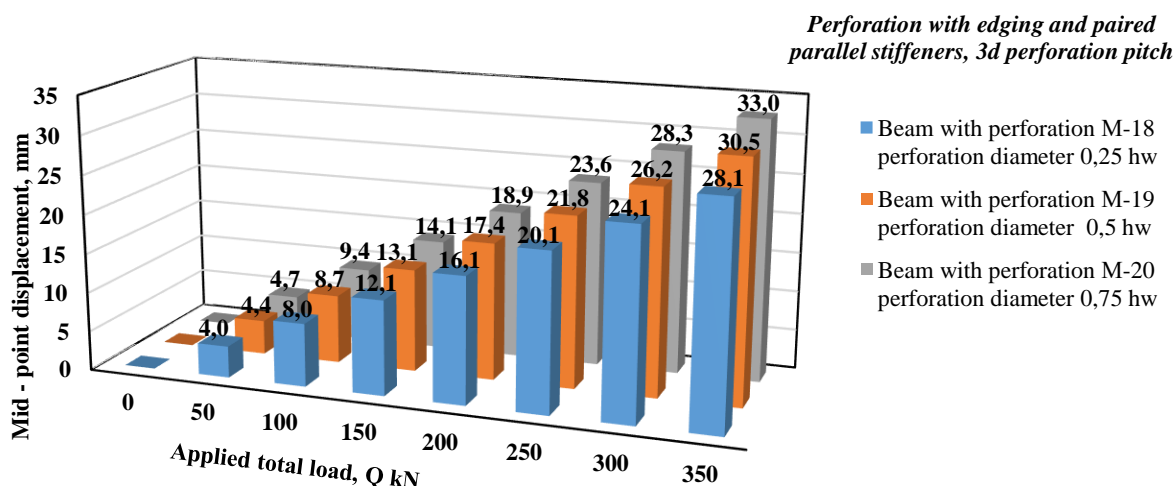


Figure 14 – The plot of displacement and applied total load value dependence for the M-18, M-19 and M-20 with 3d perforation pitch with perforation border and paired parallel stiffeners (authors' material).

The final step in strengthening the beam models with 3d perforation pitch was the incorporation of paired parallel stiffeners in the work of the perforation web stiffened with edging. The stiffener thickness was assumed to be 10 mm. For beam model M-18 with perforation diameter $0.25h_w$, stiffening with paired parallel ribs had almost no effect on its bearing capacity, but for beam models M-19 and M-20 with perforation diameters $0.5h_w$ and $0.75h_w$ showed better results.

The Figure 15 shows the load-deflection dependence of the middle of the M-21, M-22 and M-23 beam models with 4d perforation pitch in the elastic stage.

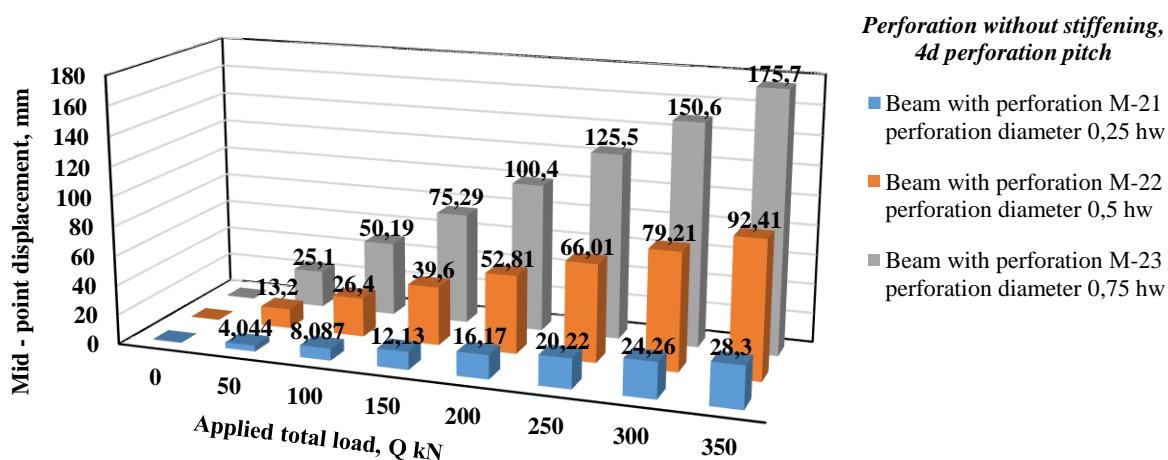


Figure 15 – The plot of displacement and applied total load value dependence for the M-21, M-22 and M-23 with 4d perforation pitch without perforation stiffening [authors' material].

Analyzing the obtained data of beam models M-21, M-22 and M-23 it can be concluded that in general the deflections and deformations of beam models with 4d perforation pitch without perforation stiffening are larger than those of similar beam models M-12, M-13, M-14 with the same perforation diameter but different perforation pitch equal to 3d and similar beam models M-3, M-4, M-5 with the same perforation diameter but different perforation pitch equal to 2d. The deformations and displacements of beam models M-21, M-12 and M-3 with perforation pitch of 4d, 3d and 2d and perforation diameter $0.25h_w$ are identical.

The Figure 16 shows the load-deflection dependence of the middle of the M-24, M-25 and M-26 beam models with 4d perforation pitch in the elastic stage.

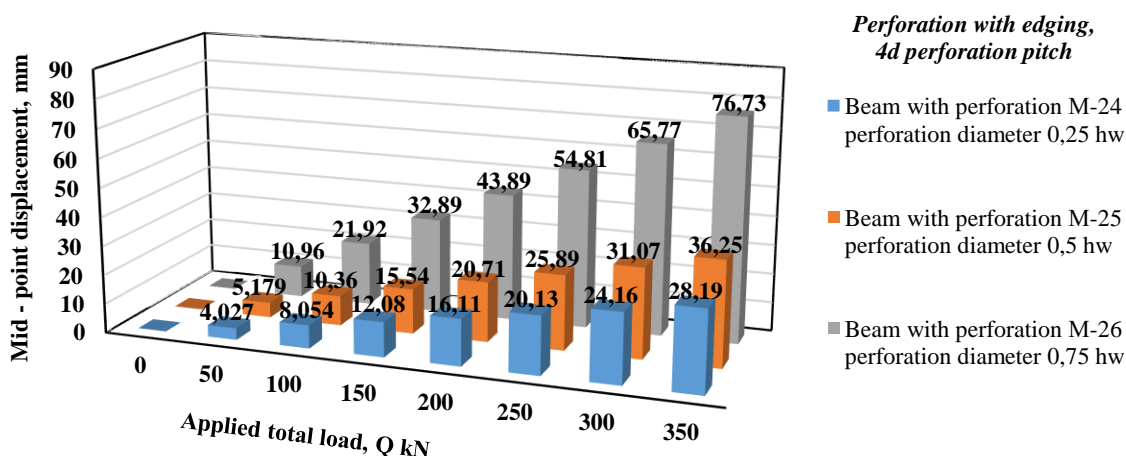


Figure 16 – The plot of displacement and applied total load value dependence for the M-24, M-25 and M-26 beam models with 4d perforation pitch with perforation edging [authors' material].

After the performance of beam models M-24, M-25 and M-26 with 4d perforation pitch with the inclusion of **perforation** stiffening by edging, the following results were obtained: as in the previous cases, the behavior of beam model M-24 with perforation diameter $0.25h_w$ and perforation pitch of 4d did not change much after stiffening and also showed almost no change compared to the data obtained for beam models M-6 and M-15 with the same diameter but perforation pitch of 2d and 3d, respectively. But for the other two models M-25 and M-26, the reinforcement by the edging had a positive effect and reduced their deflection compared to the beam models M-22 and M-23.

The **Figure 17** shows the load-deflection dependence of the middle of the M-27, M-28 and M-29 beam models with 4d perforation pitch in the elastic stage.

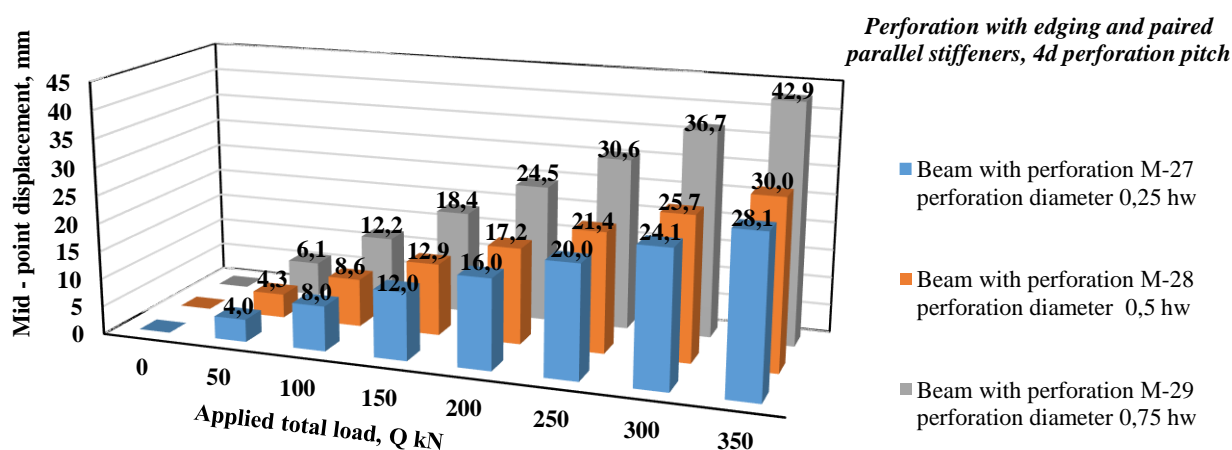


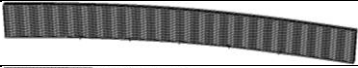















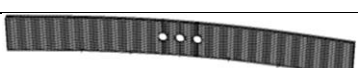
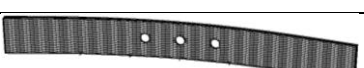











Figure 17 – The plot of displacement and applied total load value dependence for the M-27, M-28, and M-29 with 4d perforation pitch with perforation edging and paired parallel stiffeners [authors' material].

The final step in stiffening the beam models with perforation pitch 4d, as well as for perforations with spacing 2d, 3d was the inclusion of paired parallel stiffeners in the work of the web with perforations stiffened by edging. The stiffener thickness was assumed to be 10 mm. For beam model M-27 with a perforation diameter of $0.25h_w$, the reinforcement with paired ribs had almost no effect on its load carrying capacity. For beam models M-28 and M-29 with perforations of diameter $0.5h_w$ and $0.75h_w$, strengthening gave better results.

Table 1 shows the deformation shapes of beam models with different perforation diameters, with different perforation pitch under load.

Table 1 – Deflection shape of beam models with different diameters of three perforations without stiffening and with stiffening, with 2d, 3d, 4d perforation pitch.

Grade of the Model	Diameter of the perforation	Deformation shape of beam models with and without perforations	Grade of the Model	Diameter of the perforation	Deformation shape of beam models with perforation
M-1	-		M-16	$0.5h_w$	
M-2	-		M-17	$0.75h_w$	
M-3	$0.25h_w$		M-18	$0.25h_w$	
M-4	$0.5h_w$		M-19	$0.5h_w$	
M-5	$0.75h_w$		M-20	$0.75h_w$	
M-6	$0.25h_w$		M-21	$0.25h_w$	
M-7	$0.5h_w$		M-22	$0.5h_w$	
M-8	$0.75h_w$		M-23	$0.75h_w$	
M-9	$0.25h_w$		M-24	$0.25h_w$	
M-10	$0.5h_w$		M-25	$0.5h_w$	
M-11	$0.75h_w$		M-26	$0.75h_w$	
M-12	$0.25h_w$		M-27	$0.25h_w$	
M-13	$0.5h_w$		M-28	$0.5h_w$	
M-14	$0.75h_w$		M-29	$0.75h_w$	
M-15	$0.25h_w$				

According to the analysis of beam models with perforations of various diameters and pitches, the following main conclusions can be drawn:

- the most effective beam model with perforation diameter $0.25h_w$ with 2d s perforation pitch was beam model M-9, with 3d perforation pitch beam model M-18, with 4d perforation pitch beam model M-27. All the beam models whose perforations were strengthened by sheet steel edging and paired stiffening ribs located on both sides of the perforation showed the best results. For design purposes, can recommend the beam model M-9 which has the best performance with perforation diameter $0.25h_w$ and perforation pitch 2d;

- the most effective beam model with perforation diameter $0.5h_w$ with 2d spacing was the M-10 beam model, with 3d perforation pitch the M-19 beam model, and with 4d perforation pitch the M-28 beam model. All the above models, whose perforations were strengthened by sheet steel edge-

ing and paired stiffening ribs located on both sides of the perforation, showed the best results. For design purposes, can recommend the M-10 beam model which has the best performance with perforation diameter $0.5h_w$ and perforation pitch $2d$;

- the most effective beam model with perforation diameter $0.75h_w$ with $2d$ perforation pitch was beam model M-11, with $3d$ perforation pitch beam model M-18, with $4d$ perforation pitch beam model M-27. All the above models, whose perforations were strengthened by sheet steel edging and paired stiffening ribs located on both sides of the perforation, showed the best results. For design purposes, out of the above three beam models, we can recommend beam model M-11 which has the best performance with perforation diameter $0.75h_w$ and perforation pitch $2d$.

5 CONCLUSIONS

1. In this paper, was investigated operation of a welded I-beam with cross-corrugated web and triangular-shaped corrugations weakened by technological circular perforation.

2. A numerical parametric study of a beam wall with triangular corrugation outline and a thin-walled rib beam was performed, which included the analysis of 29 finite element modeled models. Out of these 29 models, 2 beam models were without perforations and 27 models had perforations in the wall structure with diameters $0.25h_w$, $0.5h_w$ and $0.75h_w$ at $2d$, $3d$ and $4d$ perforation pitch between perforation centers. The parametric study in the finite element analysis software package was carried out for beam models, considering different sizes of perforations in the beam web, perforation pitch, with and without perforation stiffening, as well as cross-corrugated web and triangular-shaped corrugations without perforation and thin-walled beam with stiffeners. The data obtained showed the effectiveness of placing perforations in the corrugated web with perforation $2d$ perforation pitch and with perforation diameters $0.25h_w$ и $0.5h_w$ stiffened with ring plates and parallel stiffeners. Thus, for the models with perforation diameter $0.5h_w$, stiffening with ring plates and parallel stiffeners increased the load carrying capacity of the beam with corrugated web weakened by technological circular perforations up to 20-25% and another 3-5% after stiffening with plate bending elements on the ring stiffener.

3. The methods of stiffening the technological circular perforation with ring plates and paired vertical stiffeners have been investigated, their influence on the operation of beam models with corrugated wall with perforations has been evaluated, as well as the influence of bending the outer edge of the ring plate on the load-bearing capacity of cross-corrugated web and triangular-shaped corrugations with perforation. The proposed methods of stiffening of technological circular perforation weakening the corrugated web of a welded I-beam have shown their effectiveness.

4. It should be noted the necessity and effectiveness of web stiffening in the areas between the belts and the element of stiffening of the perforation with paired stiffeners, in order to eliminate the loss of local stability under the concentrated load in the zone of the ring plate.

REFERENCES

1. **Bryantsev, A.A.** (2017). The effectiveness of the use of I-beams with corrugated webs in an industrial building [Effektivnost' primeneniya dvutavrov s gofrirovannymi stenkami v zdanii proizvodstvennogo naznacheniya], Construction of unique buildings and structures, 3(54), 93 – 104. <https://www.doi.org/10.18720/CUBS.54.8> (In Russ.).
2. **Poltoradnev, A.S.** (2013). Load-bearing capacity and optimization of thin-walled steel beams [Nesushchaya sposobnost' i optimizatsiya stal'nykh tonkostennykh balok], Abstract of the dissertation for the degree of Candidate of Technical Sciences, 05.23.04, Moscow. [PDF file]. Retrieved from: <https://www.dissercat.com/content/nesushchaya-sposobnost-i-optimizatsiya-stalnykh-tonkostennykh-balok> (In Russ.).
3. **Coker, E. Failon, L.** (1936). An optical method for studying stresses [Opticheskiy metod issledovaniya napryazhenij.]. [PDF file]. Retrieved from: <https://lib-bkm.ru/10053> (In Russ.).

4. **Tuzi, Z.** (1928). Scientific Papers of the Institute of Physical and Chemical Research, 156. Retrieved from: <https://catalogue.nla.gov.au/catalog/3640206>
5. **Kudryavtsev, S.V.** (2011). Load-bearing capacity of beams with a corrugated web weakened by a circular perforation [Nesushchaya sposobnost' balok s gofirovannoj stenkoj, oslablennoj krugovym otverstiem], Abstract of the dissertation for the degree of Candidate of Technical Sciences, 05.23.01, Yekaterinburg, UrFU. Retrieved from: <https://www.dissercat.com/content/nesushchaya-sposobnost-balok-s-gofirovannoi-stenkoi-oslablennoi-krugovym-otverstiem> (*In Russ.*)
6. **Chung, K.F.** (2001). Investigation on Vierendeel mechanism in steel beams with circular web openings, Journal of constructional steel research, 57, 467–490. [https://www.doi.org/10.1016/S0143-974X\(00\)00035-3](https://www.doi.org/10.1016/S0143-974X(00)00035-3)
7. **Chung, K.F.** (2003). Steel beams with large web openings of various shapes and sizes: an empirical design method using a generalized moment–shear interaction curve, Journal of constructional steel research, 59, 1177–1200. [https://www.doi.org/10.1016/S0143-974X\(03\)00029-4](https://www.doi.org/10.1016/S0143-974X(03)00029-4)
8. **Richard, R., Soon, H.Ch.**, (1993). Design of steel and composite beams with web openings, American institute of steel construction, Journal of Constructional Steel Research, 25, 23–41. [https://doi.org/10.1016/0143-974X\(93\)90050-3](https://doi.org/10.1016/0143-974X(93)90050-3)
9. **Hagen, N.C.** (2009). Shear capacity of steel plate girders with large web openings, Part 1: Modeling and simulations, Journal of constructional steel research, 65, 142–150. <https://doi.org/10.1016/j.jcsr.2008.03.014>
10. **Hagen, N.C.** (2009). Shear capacity of steel plate girders with large web openings, Part 2: Design guidelines, Journal of constructional steel research, 65, 151–158. <https://doi.org/10.1016/j.jcsr.2008.03.005>
11. **Shanmugan, N.E. Lian, V.T. Thevendran, V.** (2002). Finite element modeling of plate girders with web openings, Thin-walled structures, 40, 443–464. [https://doi.org/10.1016/S0263-8231\(02\)00008-3](https://doi.org/10.1016/S0263-8231(02)00008-3)
12. **Ahmed, M.S.** (2022). Numerical study of the effects of web openings on the load capacity of steel beams with corrugated webs, Journal of Constructional Steel Research, September 2022, 107418. <https://doi.org/10.1016/j.jcsr.2022.107418>
13. **Romeijn, A., Sarkhosh, R. and Hoop, H.** (2009). Basic parametric study on corrugated web girders with cut outs, Journal of Constructional Steel Research, 65, 395–407. <https://doi.org/10.1016/j.jcsr.2008.02.006>
14. **Kiyamaz, G., Coskun, E., Cosgun, C. and Seckin, E.** (2010). Transverse load carrying capacity of sinusoidal corrugated steel web beams with web openings, Steel and Composite Structures, 10 (1), 69–85, <https://doi.org/10.12989/scs.2010.10.1.069>
15. **Chittaranjan, N. Samadhan, M.** (2019). Comparative study of effect of web openings on the strength capacities of steel beam with trapezoidally corrugated web, Asian Journal of Civil Engineering. <https://doi.org/10.1007/s42107-019-00166-6>
16. **Amr, B.S., Sedky, A.T., Amr, E., Ahmed, A.M.** (2021). Numerical study of flange buckling behavior of high-strength steel corrugated web i-girders, JES Journal of Engineering Sciences, 49(1):85–106. <https://doi.org/10.21608/jesaun.2021.55553.1025>
17. **Ahmed, S.T., Rabiee, A.S., Amr, B.S., Ahmed A.** (2022). EL-Serwi Behavior Of Trapezoidal Corrugated Girders webs with cutouts: Experimental and Analytical Solution, JES Journal of Engineering Sciences 50 (3), <https://doi.org/10.21608/jesaun.2022.121021.1115>
18. **Bryantsev, A.A., Absimetov, V.E., Lalin, V.V.** (2019). The effect of perforations on the deformability of welded beam with corrugated webs. Magazine of Civil Engineering, 3(87):18–34, <https://www.doi.org/10.18720/MCE.87.2>
19. **Bryantsev, A.A., Absimetov, V.E.** (2020). Laboratory Tests of Welded Corrugated Beams with Perforations, Proceedings of EECE 2019, Energy, Environmental and Construction Engineering, https://www.doi.org/10.1007/978-3-030-42351-3_5